NUMERICAL BASED LINEAR MODEL FOR DIPOLE MAGNETS*

Y. Li[#], S. Krinsky, M. Rehak, BNL, Upton, NY, 11953 U.S.A.

Abstract

In this paper, we discuss an algorithm for constructing a numerical linear optics model for dipole magnets from a 3D field map. The difference between the numerical model and K. Brown's analytic approach is investigated and clarified. It was found that the optics distortion due to the dipoles' fringe focusing must be properly taken into account to accurately determine the chromaticities. In NSLS-II, there are normal dipoles with 35-mm gap and dipoles for infrared sources with 90-mm gap. This linear model of the dipole magnets is applied to the NSLS-II lattice design to match optics parameters between the DBA cells having dipoles with different gaps.

INTRODUCTION

In modern ring-based light sources, accurate optics calculation and control are key factors in achieving and improving machine performance. The accuracy of the ring lattice model depends on how well the focusing properties of individual components are modeled. Due to its complexity, dipole magnets' fringe field has been widely studied and investigated. There are several models used in optics design and nonlinear tracking study [1, 2, 3], among them K. Brown's model [1] has been widely adopted by accelerator design codes, like MAD [7], Elegant, etc. But for most existing machines, the measured optics and chromaticity are quite different from the theory calculation results based on K. Brown's model. This suggests that this model may not be accurate enough to describe the real dipole field. This work attempts to construct a dipole model directly based on its numerical field map for use in ring lattice design study.

Another motivation of this study is to control the optics mismatch of Double Bend Achromat (DBA) cells composed of different types of dipoles. A new light source, NSLS-II [4], is under construction at Brookhaven National Laboratory. The NSLS-II storage ring is composed 30 DBA cells. Among them, 27 cells will contain pairs of dipoles with 35mm gap while 3 cells will contain pairs of dipoles with 90mm gap for use as far IR sources. These two types of dipoles with different fringe field roll-off in their fringe region will lead to different lattice perturbations, such as beta-beat and tune-shift. Characterizing these two types of DBA cells and controlling their optics mismatch are important for NSLS-II lattice design.

CONSTRUCTION OF NUMERICAL LINEAR OPTICS MODEL

Our numerical dipole model is directly based on 3D magnetic field map calculated by the electromagnetic solver, Opera-3d [5]. The basic algorithm of constructing the numerical model can be described as:

- Obtain the dipole's 3D magnetic vector field from calculation. The 3D field map extends far enough in longitudinal direction to include its fringe field;
- Determine the reference orbit by tracking a nominal particle starting from the ideal orbit by integrating the differential equations of motion driven by the Lorentz force;
- Track multi-particles with different initial coordinates and record their coordinates at dipole entrance and exit;
- Extract linear transformation matrix from tracking results.

Clarification of statements above follows below: The "ideal orbit" is nominal particle trajectory passing through the ideal hard edge dipole model, namely a certain arc with a constant bending radius and two straight lines tangent to the arc. The "reference orbit" is interpreted as the ideal particle's trajectory through the real dipole field. The reference orbit should coincide with the ideal orbit at both ends well outside the fringe field region. The algorithm of tracking particles through the 3D field map is a 4th Runge-Kutta integration. There are several methods available to extract linear transformation matrices from tracking results. The easiest one is calculating its Jacobian matrix directly, but the transformation matrix obtained in this way is not strictly symplectic. In order to avoid this difficulty, multi-particle trajectories were fitted into a 4th generating function [6], and then a linear transformation matrix was extracted from it. Thus the non-symplectic integration (here Runge-Kutta integration) results will be symplectified automatically.

ANALYSIS AND COMPARISON WITH K. BROWN'S MODEL

Two coordinate systems are used for analysis as shown in Fig. 1: the 3D field maps are given in Cartesian coordinates (X, y, Z), so particle tracking is also implemented in this coordinate system. In order to extract a linear transformation matrix from tracking data, the particle's coordinates are transformed into the local coordinates (x, y, s) relative to the reference orbit at both entrance and exit points.

Considering linear terms only and using the symmetry with respect to the median plane, the relation between the two different coordinate systems can be written as:

$$\vec{e}_s(s) = \vec{e}_Z \cos\theta(s) - \vec{e}_X \sin\theta(s), \quad \vec{e}_x(s) = \vec{e}_Z \sin\theta(s) + \vec{e}_X \cos\theta(s)$$

$$\frac{d\theta(s)}{ds} = \frac{1}{\rho(s)} = \frac{1}{(B\rho)_0} B_y(s)$$

Particles linear dynamics can be described by Hill's equation

$$u'' + k_u(s)u = 0$$

Beam Dynamics and Electromagnetic Fields

u denotes here x or y, k is the normalized focusing strength. Concentrating only on the vertical plane, the normalized focusing strength can be deduced as

$$\vec{B}(s) = B_Z \vec{e}_Z + B_X \vec{e}_X + B_y \vec{e}_y$$

$$B_x(s) = B_Z \vec{e}_Z \cdot \vec{e}_x + B_X \vec{e}_X \cdot \vec{e}_x + B_y \vec{e}_y \cdot \vec{e}_x$$

$$= B_Z \sin\theta(s) + B_X \cos\theta(s)$$

$$k_y(s) = -\frac{1}{(B\rho)_0} \frac{\partial B_x(s)}{\partial y}$$

$$= -\frac{1}{(B\rho)_0} \left[\frac{\partial B_y(s)}{\partial Z} \sin\theta(s) + \frac{\partial B_y(s)}{\partial X} \cos\theta(s) \right] \qquad (1)$$

where we have used $\nabla \times \vec{B} = 0$.
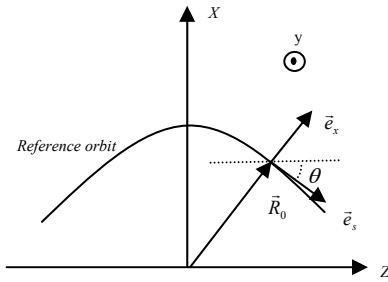
Figure 1: Two coordinates systems for dipole study.

Using the NSLS-II 35mm-gap dipole as an example, two terms in Eq. (1) were calculated and shown in Fig. 2. The first term is the projection of the bending field variation along the "longitudinal" direction (red line); the second is the projection of the bending field variation in the "transverse" plane (blue line). Here "longitudinal" and "transverse" refer to Cartesian coordinate system (X, y, and Z).
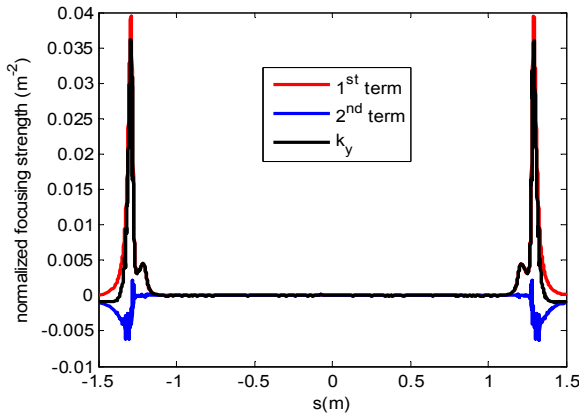
Figure 2 (Color): Linear focusing terms along logitudinal direction from Eq. (1).

In Fig. 2, the fringe field focusing range is quite narrow, its effective length can be estimated as

$$L_{fringe} = \frac{\int k_y(s) ds}{\max(k_y(s))} \approx 3.14 cm$$

So its focal length can be obtained by integrating the normalized focus strength along the longitudinal direction,

Beam Dynamics and Electromagnetic Fields

D01 - Beam Optics - Lattices, Correction Schemes, Transport

$$\int_0^s k_y ds = -\frac{1}{f_y} = -0.0029 m^{-1} \qquad (2)$$

The numerical 4×4 horizontal-vertical transformation matrix obtained by using the algorithm described in the previous section is:

$$M_{Numerical} = \begin{bmatrix} 0.9990 & 2.6023 & 0 & 0 \\ -0.0008 & 0.9988 & 0 & 0 \\ 0 & 0 & 0.9962 & 2.6151 \\ 0 & 0 & -0.0029 & 0.9963 \end{bmatrix} \qquad (3)$$

It can be seen that the vertical focusing term M_{43} in Eq. (3) is in excellent agreement with Eq. (2).

K. Brown's model uses a thin lens to describe the fringe field, and introduces a modification factor when the soft-edge effect has been taken into account [1]. A 4×4 horizontal-vertical transformation matrix obtained by using his formulae [1] is:

$$M_{K\_Brown} = \begin{bmatrix} 1 & 2.6152 & 0 & 0 \\ 0 & 1 & 0 & 0 \\ 0 & 0 & 0.9946 & 2.62 \\ 0 & 0 & -0.0041 & 0.9946 \end{bmatrix} \qquad (4)$$

Comparison with Eq. (3) shows the vertical focusing terms M_{43} differ significantly. This is because the $\frac{\partial B_y}{\partial X}$ term in Eq. (1) must be included.

One cell of the NSLS-II DBA lattice is used to compare the optics difference by using these two models. We use lattice design code MAD [7] to calculate Twiss parameters. The calculated Twiss parameters are shown in Fig. 3. Obvious differences (~10%) can be observed in the vertical plane. The difference of chromaticities calculation will be investigated in the next section.
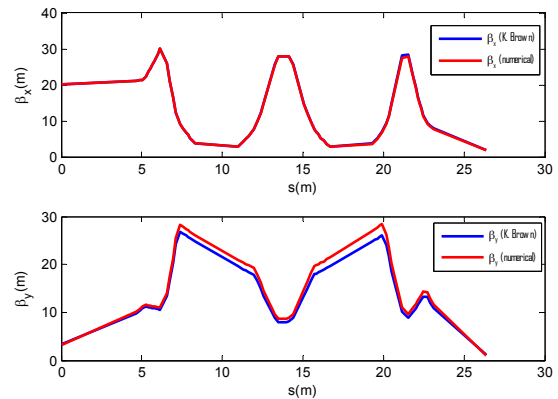
Figure 3 (Color): One cell optics parameters of NSLS-II by using different dipole models.

In fact, it can be proven (not shown here) that the integral of the first term in Eq. (1) is approximately equal to $\int_0^L \frac{1}{\rho^2} ds$ under the condition that bending angle θ is small enough. A Further simplification:

$$\int_0^L \frac{1}{\rho^2(s)} ds \approx \frac{1}{\rho}\int_0^L \frac{1}{\rho} ds = \frac{2\theta_0}{\rho} \approx \frac{2}{\rho}\tan\theta_0$$

shows it is the first order term in K. Brown's model. The second defocusing term in Eq. (1), which comes from the fringe field "transverse" gradient, isn't negligible here. We need to include it into our linear optics design consideration in order to get correct optics parameters.

The analysis for the horizontal plane can be implemented in the same way; however the bend focusing needs to be included inside the dipole body, which can't be treated as a thin lens any longer. The matrix in Eq. (3) can be expanded into a 6×6 matrix by tracking particles with different energy deviations.

From Eq. (1), we see that the fringe field effect can be derived from the vertical component on the median plane in Cartesian coordinates. It is a consequence of Maxwell's equations, and suggests an easy way to determine the dipole fringe focusing effects by using Hall probe technique to measure only the dominant field component.

CHROMATICITIY CALCULATION

The dipole fringe field contribution to chromaticity can be found in refs. [8, 9, 10].

$$\frac{\partial \nu_x}{\partial \delta} = \frac{1}{4\pi}\int_0^L \left\{\beta_x\left[\left(-k_x - h_x^2\right) + 2k_x h_x \eta_x\right] - 2\alpha_x \eta_x' h_x' + \gamma_x h_x \eta_x\right\} ds$$

$$\frac{\partial \nu_y}{\partial \delta} = \frac{1}{4\pi}\int_0^L \left\{\beta_y\left[-k_y + k_y h_x \eta_x + h_x' \eta_x'\right] + \gamma_y h_x \eta_x\right\} ds$$

Here, $h_x = \frac{1}{\rho}$, $' = \frac{\partial}{\partial s}$, α, β, γ are Twiss parameters and η_x is the horizontal dispersion. After inserting the numerical matrices into MAD code, the optics parameters on both ends of magnet are obtained. Using the known values for $k_{x,y}(s)$ and the expressions of the derivatives of the Twiss parameters [11],

$$\beta' = -2\alpha, \quad \alpha' = k\beta - \gamma, \quad \text{and } \gamma' = 2k\alpha,$$

Twiss parameters inside dipole along the longitudinal direction can be determined. Thus the integrations along the reference orbit can be calculated as $\partial\nu_x/\partial\delta = 0.012$, $\partial\nu_y/\partial\delta = -0.0012$ for one dipole, the total contribution from all 60 dipoles is 0.72 and -0.07, respectively. Although the direct contributions from the dipoles are quite small, obvious difference appear by comparing the chromaticities calculation results by using these two dipole models, especially in the vertical plane. The reason is that the dipole fringe field's focus strength is overestimated in K. Brown's model (see Eq. (3) and (4)), yielding results smaller than actual values, and at the same time, the chromaticity is proportional to the beta function at quadrupoles locations. This eventually causes the actual vertical chromaticity to be larger than the calculation results of K. Brown's model. For example, NSLS-II lattice using K Brown's dipole model gives $\xi_{x/y} = -101.2/-40.5$, while using the numerical model gives $\xi_{x/y} = -100.0/-43.6$. For small rings with large dipole fringe angle and wide fringe field region, this difference could become even more dramatic.

APPLICATION

This numerical dipole model is used in NSLS-II lattice design to match the DBA cells with different types of dipoles (with a gap of 35mm and 90mm). The quadrupole triplets in the long and short straight sections are chosen to match the optics to desired boundary values at the centre of two straight sections. Fig. 4 shows the optics parameters after the quadrupole K-values have been re-adjusted. In this way, the optics difference between different DBA cells can be controlled better than 1%.
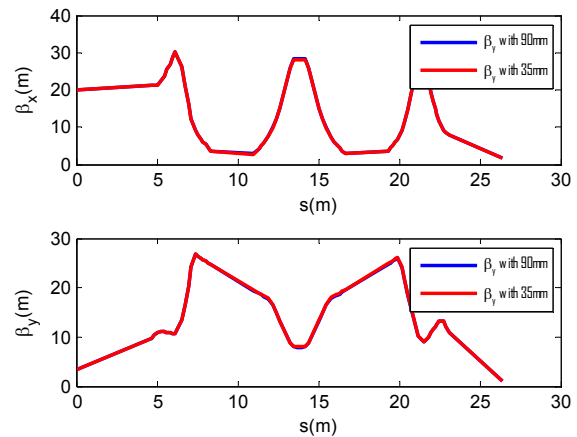
Figure 4 (Color): One cell optics parameters of NSLS-II after using quadrupoles triplets to re-match optics.

SUMMARY

An algorithm for constructing a numerical linear model for a dipole magnet is developed. This numerical model can bridge between the physics model and the magnet's design and measurement. It also provides a guide to dipole design at its inception. Inclusion of nonlinear terms from dipole fringe field is under study.

REFERENCES

[1] K. Brown, SLAC-75 (1967)
[2] M. Berz et al, Phys. Rev. ST-AB, 124001 (2000)
[3] E. Forest et al, KEK-PREPRINT-2005-110 (2006)
[4] NSLS-II Preliminary Design Report, http://www.bnl.gov/nsls2/project/PDR/
[5] Opera 3D, http://www.vectorfields.com/
[6] M. Scheer, BESSY-TB 92-169-B (1992)
[7] H. Grote et al, CERN/SL/90-13-AP (1994)
[8] W. Hardt et al, PS-LEA-Note 82-5 (1982)
[9] M. Bassetti, LEP-Note-504 (1984)
[10] H. Wiedemann, Part. Acc. Phys., 3rd, Springer (2006)
[11] E. Courant et al, Ann. Phys. 3, 1 (1958)